Retrieval and analysis of a polarized high-spectral-resolution lidar for profiling aerosol optical properties

Dong Liu,* Yongying Yang, Zhongtao Cheng, Hanlu Huang, Bo Zhang, Tong Ling, and Yibing Shen

State Key Lab of Modern Optical Instrumentation, Zhejiang University, Hangzhou, Zhejiang 310027, China
*liudongopt@zju.edu.cn

Abstract: Taking advantage of the broad spectrum of the Cabannes-Brillouin scatter from atmospheric molecules, the high spectral resolution lidar (HSRL) technique employs a narrow spectral filter to separate the aerosol and molecular scattering components in the lidar return signals and therefore can obtain the aerosol optical properties as well as the lidar ratio (i.e., the extinction-to-backscatter ratio) which is normally selected or modeled in traditional backscatter lidars. A polarized HSRL instrument, which employs an interferometric spectral filter, is under development at the Zhejiang University (ZJU), China. In this paper, the theoretical basis to retrieve the aerosol lidar ratio, depolarization ratio and extinction and backscatter coefficients, is presented. Error analyses and sensitivity studies have been carried out on the spectral transmittance characteristics of the spectral filter. The result shows that a filter that has as small aerosol transmittance (i.e., large aerosol rejection rate) and large molecular transmittance as possible is desirable. To achieve accurate retrieval, the transmittance of the spectral filter for molecular and aerosol scattering signals should be well characterized.

©2013 Optical Society of America

OCIS codes: (010.0010) Atmospheric and oceanic optics; (120.0280) Remote sensing and sensors; (280.3640) Lidar; (280.1350) Backscattering; (120.4640) Optical instruments; (120.3180) Interferometry.

References and links

1. CCSP, 2009: Atmospheric aerosol properties and climate impacts, A report by the U.S. Climate Change Science Program and the Subcommittee on Global Change Research. [Mian Chin, Ralph A. Kahn, and Stephen E. Schwartz (eds.)]. National Aeronautics and Space Administration, Washington, D.C., USA, 128 pp.
2. C. Weitkamp, ed., Lidar: range-resolved optical remote sensing of the atmosphere, the Springer Series in Optical Sciences (Springer Science + Business Media Inc., Singapore, 2005).
3. S. T. Shipley, D. H. Tracy, E. W. Eloranta, J. T. Trauger, J. T. Sroga, F. L. Roesler, and J. A. Weinman, "High spectral resolution lidar to measure optical scattering properties of atmospheric aerosols. 1: theory and instrumentation," Appl. Opt. **22**(23), 3716–3724 (1983).
4. D. Liu, C. Hostetler, I. Miller, A. Cook, R. Hare, D. Harper, and J. Hair, "Tilted pressure-tuned field-widened Michelson interferometer for high spectral resolution lidar," in Optical Sensing and Detection Ii, F. Berghmans, A. G. Mignani, and P. DeMoor, eds. (2012).
5. H. Shimizu, S. A. Lee, and C. Y. She, "High spectral resolution lidar system with atomic blocking filters for measuring atmospheric parameters," Appl. Opt. **22**(9), 1373–1381 (1983).
6. C. Y. She, R. J. Alvarez II, L. M. Caldwell, and D. A. Krueger, "High-spectral-resolution Rayleigh-Mie lidar measurement of aerosol and atmospheric profiles," Opt. Lett. **17**(7), 541–543 (1992).
7. P. Piironen and E. W. Eloranta, "Demonstration of a high-spectral-resolution lidar based on an iodine absorption filter," Opt. Lett. **19**(3), 234–236 (1994).
8. Z. Liu, I. Matsui, and N. Sugimoto, "High-spectral-resolution lidar using an iodine absorption filter for atmospheric measurements," Opt. Eng. **38**(10), 1661–1670 (1999).
9. D. S. Hoffman, K. S. Repasky, J. A. Reagan, and J. L. Carlsten, "Development of a high spectral resolution lidar based on confocal Fabry-Perot spectral filters," Appl. Opt. **51**(25), 6233–6244 (2012).

#188635 - $15.00 USD Received 10 Apr 2013; revised 15 May 2013; accepted 16 May 2013; published 21 May 2013

10. J. W. Hair, C. A. Hostetler, A. L. Cook, D. B. Harper, R. A. Ferrare, T. L. Mack, W. Welch, L. R. Izquierdo, and F. E. Hovis, "Airborne high spectral resolution lidar for profiling aerosol optical properties," Appl. Opt. **47**(36), 6734–6752 (2008).
11. D. Liu, C. Hostetler, I. Miller, A. Cook, and J. Hair, "System analysis of a tilted field-widened Michelson interferometer for high spectral resolution lidar," Opt. Express **20**(2), 1406–1420 (2012).
12. J. T. Sroga, E. W. Eloranta, S. T. Shipley, F. L. Roesler, and P. J. Tryon, "High spectral resolution lidar to measure optical scattering properties of atmospheric aerosols. 2: calibration and data analysis," Appl. Opt. **22**(23), 3725–3732 (1983).
13. D. Liu, I. Miller, C. Hostetler, A. Cook, and J. Hair, "System optimization of a field-widened Michelson interferometric spectral filter for high spectral resolution lidar," in International Symposium on Photoelectronic Detection and Imaging 2011: Laser Sensing and Imaging, International Symposium on Photoelectronic Detection and Imaging 2011: Laser Sensing and Imaging (SPIE, 2011), 81924N.
14. A. Bucholtz, "Rayleigh-scattering calculations for the terrestrial atmosphere," Appl. Opt. **34**(15), 2765–2773 (1995).
15. C.-Y. She, "Spectral structure of laser light scattering revisited: bandwidths of nonresonant scattering lidars," Appl. Opt. **40**(27), 4875–4884 (2001).
16. B. A. Bodhaine, N. B. Wood, E. G. Dutton, and J. R. Slusser, "On Rayleigh optical depth calculations," J. Atmos. Ocean. Technol. **16**(11), 1854–1861 (1999).
17. J. W. Hair, L. M. Caldwell, D. A. Krueger, and C.-Y. She, "High-spectral-resolution lidar with iodine-vapor filters: measurement of atmospheric-state and aerosol profiles," Appl. Opt. **40**(30), 5280–5294 (2001).
18. D. Bruneau and J. Pelon, "Simultaneous measurements of particle backscattering and extinction coefficients and wind velocity by lidar with a Mach-Zehnder interferometer: principle of operation and performance assessment," Appl. Opt. **42**(6), 1101–1114 (2003).

1. Introduction

Quantitative measurements of atmospheric aerosol optical properties are required for studies of the Earth's radiation budget and climate change [1]. Backscatter lidars are widely used to measure atmospheric aerosols. In the data processing of backscatter lidars, however, the extinction-to-backscatter ratio (or the lidar ratio) has to be assumed to be a constant and known in order to solve the 'one-equation, two-unknown' problem to retrieve aerosol optical properties. The retrieval accuracy of backscatter lidars is therefore limited by the accuracy of lidar ratio selection. In reality, however, the lidar ratio can vary in a large range for the atmospheric aerosols depending on their composition, size distribution, shapes and refractive index [2].

Taking advantage of the broad spectrum of the Cabannes-Brillouin scattering from atmospheric molecules, the high spectral resolution lidar (HSRL) technique employs a narrow spectral filter to reject the aerosol Mie scattering component in the lidar return signals. Therefore, an HSRL can directly measure the extinction and backscatter coefficient as well as the lidar ratio [3–5]. Numerous HSRL systems employing either atomic/molecular absorption filter [5–8] or Fabry-Perot interferometer (FPI) [3,9] have been built. An absorption filter can suppress the aerosol scattering by a factor of at least 10^{-5}. The retrieval process is simple as the residual Mie scattering in the output signal from the filter is ignorably small and hence no additional correction is needed [10]. Unlike the absorption filter, an interferometric filter produces two complementary outputs, and can only suppress the aerosol signal by a factor of about 10^{-1} to 10^{-3} [11–13]. Because there is a significant amount of residual Mie scattering left in the filtered signal, correction is employed to deal with the cross talk between the two outputs of the filter.

A polarized HSRL instrument, which employs an interferometric spectral filter, is under development at the Zhejiang University (ZJU), China. In this paper, the retrieval of the aerosol optical properties, such as extinction-to-backscatter ratio and aerosol depolarization ratio, is presented. Sensitivity of the aerosol retrieval to errors in characterizing the transmittance of the molecular and aerosol scattering signal of the spectral filter is also investigated.

The paper is constructed as follow. Section 2 presents the layout of the ZJU polarized HSRL system. Section 3 presents the mathematical basis to retrieve the aerosol optical

#188635 - $15.00 USD Received 10 Apr 2013; revised 15 May 2013; accepted 16 May 2013; published 21 May 2013
(C) 2013 OSA

properties. Error analyses of the aerosol retrieval are performed in Section 4, which is followed by the conclusions of this paper in Section 5.

2. ZJU polarized high spectral resolution lidar

2.1 General description of interferometric HSRL

An HSRL takes advantage of the broad spectrum of the Cabannes-Brillouin scattering from atmospheric molecules and employs a narrow spectral filter to separate the molecular component from the aerosol component which has a much narrower spectrum in the lidar return signal. The spectral transmission function of an HSRL using an interferometric filter is schematically illustrated in Fig. 1, where Fig. 1(a) shows the spectral transmission of the HSRL interferometric filter and Fig. 1(b) shows the molecular and aerosol components in the output spectrum of the filter. In Fig. 1(a), the black dashed curve is the atmosphere backscatter signal while the pink solid and turquoise solid curves are the backscatter transmission and output signal from the spectral filter, respectively. The detected atmospheric backscatter signal is composed of a narrow spike from aerosols superimposed on a broad Gaussian-like distribution from molecules. The laser used in an HSRL system is quasi-monochromatic and has very narrow spectrum. When the laser is transmitted into the atmosphere, the scattered lights will be Doppler broadened by the random motion of the atmospheric aerosols or molecules. Because the Doppler broadening in the aerosol backscatter spectrum for a monochromatic source is 1-2 orders in magnitude smaller than the transmitter bandwidth, the aerosol backscatter spectral distribution is essentially the same as the laser spectral distribution. In contrast, the molecular signal is very broad and is about some GHz wide depending on the temperature and working wavelength. Both signals distribute in a Gaussian-like shape and center at the central frequency of the laser, as illustrated in Fig. 1(a). As is indicated, an interferometric filter produces two complementary outputs. Usually, the valley of one transmission curve is chosen to locate at the central frequency of the laser, thus suppressing the aerosol scattering. As is shown in Fig. 1(a), the output spectrum mainly contains the molecular scattering signal while the aerosol component is hardly to find.

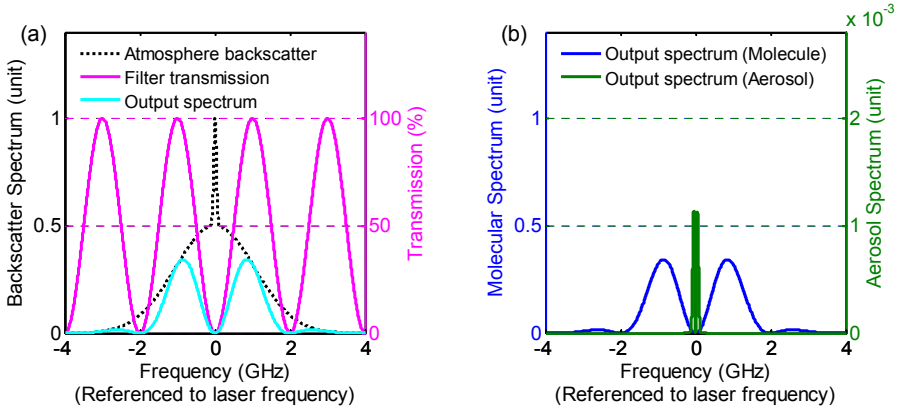

Fig. 1 Schematic illustration of the spectral transmission of the HSRL spectral filter, (a) the spectral transmission in the HSRL interferometric filter, (b) the molecular and aerosol components in the output spectrum of the filter.

Note that, the filter transmission function in Fig. 1(a) is idealized. Yet even that, because of the nature of interferometric filters, the aerosol scattering cannot be blocked totally and there is still some remaining in the transmitted signal. Figure 1(b) shows the molecular (blue) and aerosol (green) components of the output spectrum of the interferometric filter, respectively. We can find that, there is some aerosol scattering signal left in the output spectrum. In contrast to the absorption filters that can suppress the aerosol scattering by a

#188635 - $15.00 USD Received 10 Apr 2013; revised 15 May 2013; accepted 16 May 2013; published 21 May 2013
(C) 2013 OSA

factor of at least 10^{-5}, the interferometric filter can only suppress the aerosol signal by a factor of about 10^{-1} to 10^{-3}. As a result, correction should be employed in the retrieval process to deal with the cross talk between the aerosol and molecular components in the output spectrum.

2.2 System layout

A schematic layout of the ZJU polarized HSRL system is shown in Fig. 2. The quasi-monochromatic laser is transmitted into the atmosphere and scattered by the molecules and aerosol particles in the atmosphere. The backscattered signals [2,14] from the molecules and aerosols are then collected by the telescope of the HSRL receiver. After some pre-processing optical systems, the backscatter signal is then split by a polarized beam splitter, PBS, into two orthogonally polarized beams. The reflected beam is polarized perpendicularly to the polarization direction of transmitted laser beam, called the *combined perpendicular channel beam*, which is recorded by a photomultiplier tube (PMT), PMT1. The transmitted beam is polarized parallelly, and is further split by a beam splitter, BS. Note that, BS is not a 50%:50% beam splitter but one with very small reflectance and very large transmittance. The reflected part by BS is recorded by PMT2 and called the *combined parallel channel beam*, while the transmitted part is then guided into the interferometric spectral filter. The filtered signal is collected by PMT3 and called the *molecular channel signal*.

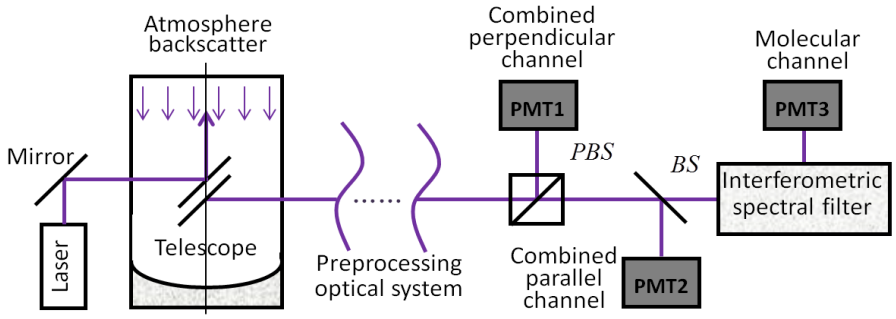

Fig. 2. Schematic layout of the polarized high spectral resolution lidar system

Note that, the ZJU polarized HSRL is just a traditional polarized lidar added with an interferometric spectral filter. As mentioned earlier, traditional backscatter lidars encounter problems of one equation with two unknowns, which makes difficult in retrieving the aerosol optical properties. With the aid of the spectral filter, additional measurements can be made and therefore the 'one-equation, two-unknown' problem can be solved. In the next section, the retrieval process of the aerosol optical properties in the ZJU polarized HSRL will be described in detail.

3. Retrieval of aerosol optical properties

The signal in the *combined perpendicular channel* and *combined parallel channel* of the ZJU polarized HSRL shown in Fig. 2 can be presented as

$$P_C^{\perp} = \frac{C_C^{\perp}}{r^2}\Psi(\beta_m^{\perp} + \beta_a^{\perp})\exp(-2\tau), \tag{1a}$$

and

$$P_C^{\parallel} = \frac{C_C^{\parallel}}{r^2}\Psi(\beta_m^{\parallel} + \beta_a^{\parallel})\exp(-2\tau), \tag{1b}$$

#188635 - $15.00 USD Received 10 Apr 2013; revised 15 May 2013; accepted 16 May 2013; published 21 May 2013
(C) 2013 OSA

respectively. The output signal of the spectral filter (*molecular channel*) is given by

$$P_M^{\parallel} = \frac{C_M^{\parallel}}{r^2}\Psi(T_m\beta_m^{\parallel} + T_a\beta_a^{\parallel})\exp(-2\tau). \tag{1c}$$

In the above equations, $C_{\mathrm{C}}^{\parallel}$, $C_{\mathrm{C}}^{\perp}$ and $C_{\mathrm{M}}^{\parallel}$ are the system constants for the combined parallel and perpendicular channels and the molecular channel, respectively. Subscriptions M and C represent the *molecular channel* and *combined channel*s, respectively, and superscriptions $\parallel$ and $\perp$ indicate the parallel and perpendicular polarization, respectively; r is the range of the scatter volume from the lidar; Ψ is the transmitter-receiver geometric overlap function and approaches unity as the range from the lidar increases; β_m and β_a are the volume backscatter coefficients for the molecule and aerosols, respectively; T_m and T_a are the transmittance of the spectral filter for the molecular and aerosol scattering, respectively, and are determined by

$$\begin{cases} T_m = \int s_m^{\parallel}(v)t_M(v)dv \\ T_a = \int s_a^{\parallel}(v)t_M(v)dv \end{cases} \tag{2}$$

where, $s_m^{\parallel}$ and $s_a^{\parallel}$ are the spectral function of the parallel components of the atmospheric molecular and aerosol backscattering, respectively, and t_M is the transmission function of the spectral filter; τ is the optical depth as

$$\tau = \int_0^r \alpha(\xi)d\xi = \int_0^r [\alpha_a(\xi) + \alpha_m(\xi)]d\xi, \tag{3}$$

where, α_a is the aerosol extinction coefficient, and α_m is the molecular extinction coefficient and can be derived from the modeled or sonde-derived molecular density profile, N, and the total molecular extinction cross section, σ [15], as

$$\alpha_m = N\sigma. \tag{4}$$

Introducing attenuated backscatter $B = Pr^2/(C\Psi)$, i.e., the normalized, range and geometric overlap-corrected lidar return signals, Eqs. (1a) – (1c) can be rewritten as

$$B_C^{\perp} = (\beta_m^{\perp} + \beta_a^{\perp})\exp(-2\tau), \tag{5a}$$

$$B_C^{\parallel} = (\beta_m^{\parallel} + \beta_a^{\parallel})\exp(-2\tau), \tag{5b}$$

and

$$B_M^{\parallel} = (T_m\beta_m^{\parallel} + T_a\beta_a^{\parallel})\exp(-2\tau). \tag{5c}$$

This is a three-unknown ($\beta_a^{\perp}$, $\beta_a^{\parallel}$ and τ) and three-equation problem, and we can solve the equations and derive these unknowns. Taking ratio of Eqs. (5b) and (5c) and solving the resultant equation, we can derive the parallel component of the aerosol backscatter coefficient

$$\beta_a^{\parallel} = \beta_m^{\parallel}\left[\frac{(T_m - T_a)K}{1 - T_aK} - 1\right] = \frac{\beta_m}{1+\delta_m}\left[\frac{(T_m - T_a)K}{1 - T_aK} - 1\right], \tag{6}$$

where $K = B_C^{\parallel}/B_M^{\parallel}$, the volume backscatter coefficients for the molecule, β_m, can be determined from an assimilation model or radiosonde data, and $\delta_m \equiv \beta_m^{\perp}/\beta_m^{\parallel}$ is the molecular scattering depolarization ratio and normally has a value smaller than few percent. Substituting

#188635 - $15.00 USD Received 10 Apr 2013; revised 15 May 2013; accepted 16 May 2013; published 21 May 2013
(C) 2013 OSA

Eq. (6) into Eq. (5b) and then taking ratio of Eqs. (5a) and (5b), we can then derive the perpendicular component of the aerosol backscatter coefficient as

$$\beta_a^{\perp} = \frac{\beta_m}{1+\delta_m}\left[\frac{(T_m - T_a)K\delta}{1-T_aK} - \delta_m\right], \tag{7}$$

where

$$\delta = \frac{\beta_m^{\perp} + \beta_a^{\perp}}{\beta_m^{\parallel} + \beta_a^{\parallel}} = \frac{B_C^{\perp}}{B_C^{\parallel}} \tag{8}$$

is the volume depolarization ratio of the return signal including both molecular and aerosol scattering. We can further derive the aerosol backscatter coefficient as

$$\beta_a = \beta_a^{\perp} + \beta_a^{\parallel} = \beta_m\left[\frac{(1+\delta)}{(1+\delta_m)}\frac{(T_m - T_a)K}{1-T_aK} - 1\right], \tag{9}$$

and the aerosol depolarization ratio can be got readily by using

$$\delta_a \equiv \beta_a^{\perp} / \beta_a^{\parallel}. \tag{10}$$

Substituting Eq. (6) into Eq. (5c), we can obtain the optical depth from the lidar to the atmosphere at *r*,

$$\tau = -\frac{1}{2}\ln\left[\frac{(1-\mathrm{K}T_a)(1+\delta_m)B_M^{\parallel}}{(T_m - T_a)\beta_m}\right]. \tag{11}$$

The aerosol extinction coefficient and extinction-to-backscatter ratio (lidar ratio) can be readily obtained using

$$\alpha_a = \frac{\partial \tau}{\partial r} - \alpha_m, \tag{12}$$

and

$$S_a = \alpha_a / \beta_a. \tag{13}$$

From the retrieval process above we can find that, in contrast to traditional backscatter lidars, the HSRL technique can obtain the optical properties of the aerosols without assumptions of their conditions. With the aid of the spectral filter, more measurements can be made. The aerosol backscatter coefficient, β_a, the aerosol extinction coefficient, α_a, the aerosol depolarization ratio, δ_a, and the lidar ratio (extinction-to-backscatter ratio), S_a, can all be retrieved from the lidar return signals, the transmission constants of the filter, and the well-known Rayleigh scattering properties of the atmospheric gas composition [16].

4. Analysis and discussions

In the previous section, the mathematical basis to retrieve the aerosol scattering properties from the ZJU polarized HSRL have been presented. And we can conclude that the measurement accuracy of the HSRL is affected by a) the detected lidar return signals, b) the transmission characteristics of the filter, and c) the optical properties of the atmosphere molecules. Since factors (a) and (c) can be assured by choosing of high SNR (signal-to-noise ratio) detectors and more accurate atmosphere models [17], respectively, only factor (b)

#188635 - $15.00 USD Received 10 Apr 2013; revised 15 May 2013; accepted 16 May 2013; published 21 May 2013
(C) 2013 OSA

remains to be investigated. In this section we will perform error analysis and examine the sensitivity of the retrieval to the transmission constants of the filter.

From Eqs. (9) and (11),we can get the relationship between volume backscatter coefficient, β and optical depth τ as

$$\beta = \frac{(1+\delta)B_M^{\parallel}}{\exp(-2\tau)}. \tag{14}$$

Then through the derivative of β with respect to τ, we have

$$\Delta\tau = \frac{1}{2}\frac{\Delta\beta}{\beta}. \tag{15}$$

It is very interesting to find that the *absolute uncertainties* of optical depth are half the *relative uncertainties* of backscatter coefficient.

In fact, this relation can also be got from the lidar equation from a mathematical view. From Eqs. 5(a) and 5(b) we can get the lidar equation

$$B_C^{\perp}+B_C^{\parallel} = \beta\exp(-2\tau), \tag{16}$$

where, $B_C^{\perp}$ and $B_C^{\parallel}$ are the normalized, range and geometric overlap-corrected lidar return signals, β is the volume backscatter coefficient of the atmosphere, and τ is the optical depth from lidar to the measured volume atmosphere. Eq. (16) describes the relation between the factors of the lidar setup, and the power received and the atmosphere examined. One can note that since the measured signal $B_C^{\perp}$ and $B_C^{\parallel}$ can be regarded as constants, β and $\exp(-2\tau)$ play parallel roles in attenuating the laser power. In more detail, the backscatter coefficient, β, describes the ability of the atmosphere to scatter light back into the direction from which it comes while the transmission term, $\exp(-2\tau)$, shows how much light gets lost on the way from the lidar to height r and back. So we can conclude that these two terms have the same relative variations when subjecting to system parameter changes and that is

$$\frac{\Delta\beta}{\beta} = -\frac{\Delta\exp(-2\tau)}{\exp(-2\tau)}. \tag{17}$$

Using an obvious math formulation $\Delta\ln(x) = \ln(x+\Delta x) - \ln(x) \approx \Delta x / x$ and substituting $\exp(-2\tau)$ for x, we have

$$\Delta(-2\tau) = \frac{\Delta\exp(-2\tau)}{\exp(-2\tau)}. \tag{18}$$

Comparing Eqs. (17) and (18) we can obtain the same conclusion with that from Eq. (16). Since the optical depth, τ, is dependent of its value from lidar to the atmosphere at r while the backscatter coefficient is not, the relative uncertainty of the optical depth can only be obtained after the measurement is made while the relative uncertainty of the backscatter coefficient can be obtained without dependence of the value at other distance.

We introduce the parallel aerosol scattering ratio $R^{\parallel} = (\beta_a^{\parallel} + \beta_m^{\parallel})/\beta_m^{\parallel}$, which is analogue to the aerosol scattering ratio $R = (\beta_a + \beta_m)/\beta_m$ [18], then have

#188635 - $15.00 USD Received 10 Apr 2013; revised 15 May 2013; accepted 16 May 2013; published 21 May 2013
(C) 2013 OSA

$$R^{\parallel} = \frac{(T_m - T_a)K}{1 - T_a K} \quad . \tag{19}$$

The relative uncertainty in the volume backscatter coefficient ($\beta = \beta_a + \beta_m$) due to the determination error in the spectral filter constants, ΔT_a and ΔT_m, can be estimated using

$$\begin{cases} \eta_\beta^{T_a} = \dfrac{\partial \beta}{\beta \partial T_a} \Delta T_a = \dfrac{\mathrm{K}T_m - 1}{(1 - \mathrm{K}T_a)(T_m - T_a)} \Delta T_a = \dfrac{R^{\parallel} - 1}{(T_m - T_a)} \Delta T_a \\ \eta_\beta^{T_m} = \dfrac{\partial \beta}{\beta \partial T_m} \Delta T_m = \dfrac{1}{T_m - T_a} \Delta T_m \end{cases} \quad . \tag{20}$$

Figure 3 shows the relative uncertainties in the backscatter coefficient estimated using Eq. (20). In Fig. 3(a) eight cases of combination of filter transmittances T_a = 0.01 and 0.05 and T_m = 0.3 and 0.7 and aerosol transmittance errors ΔT_a = 3% and 10% (ΔT_m = 0) are examined. The calculation results for T_a = 0.05 and 0.01 are colored with blue and red, respectively, while the results for T_m = 0.3 and 0.7 are marked with "+" and "□", respectively. In general, $\eta_\beta^{T_a}$ shows an increasing dependence on $R^{\parallel}$. For low aerosol loading conditions, there is little aerosol scattering in the detected return signals. In this case, the T_a determination error does not cause significant impact on the measurement result. However, as the aerosol loading increases, ΔT_a increases its impacts on the retrieval accuracy. When T_m = 0.3, T_a = 0.01 and ΔT_a = 10%, the relative measurement uncertainty of the volume backscatter coefficient is smaller than 0.1% for $R^{\parallel}$ = 1.1 and larger than 30% for $R^{\parallel}$ = 100.

From Fig. 3(a) we can also find that, a smaller T_a and larger T_m tend to produce better retrieval accuracy. A smaller T_a value corresponds to a situation where there is a smaller fraction of the aerosol signal in the molecular channel that needs to be corrected and therefore the determination error in T_a causes smaller error in the retrieval. Similarly, a larger T_m value indicates the molecular channel is more dominated by the molecular signal and the determination error in T_a will have smaller effect on the retrieval. Note that, the analysis present here is of general meaning and can be applied to all configurations of spectral filters.

It can also be seen in Fig. 3(a), as expected, that a better determination of T_a can produce a better retrieval accuracy for the same T_a and T_m values. However, it is worthy to note that the case of T_a = 0.01 and ΔT_a = 10% produces better result than the case of T_a = 0.05 and ΔT_a = 3%. This implies that a small T_a is desired.

The backscatter coefficient retrieval error resulted from the T_m determination error is presented in Fig. 3(b). As in Fig. 3(a), we assume T_a = 0.05 or 0.01, and T_m = 0.3 or 0.7. Two error values of ΔT_m = 1% and 3% (ΔT_a = 0) are examined for each condition. Unlike the simulation results for $\eta_\beta^{T_a}$ in Fig. 3(a), the retrieval error resulted by the uncertainty in T_m remains the same for different aerosol loading conditions. Similar to the $\eta_\beta^{T_a}$ simulation in Fig. 3(a), the spectral filter with smaller T_a and larger T_m is less sensitive to the transmittance determination error and can produce better retrieval. The resultant uncertainties range from 1% to 4%. Compared with ΔT_a, ΔT_m has much smaller impact on the retrieval when the aerosol loading is large [11].

#188635 - $15.00 USD Received 10 Apr 2013; revised 15 May 2013; accepted 16 May 2013; published 21 May 2013
(C) 2013 OSA

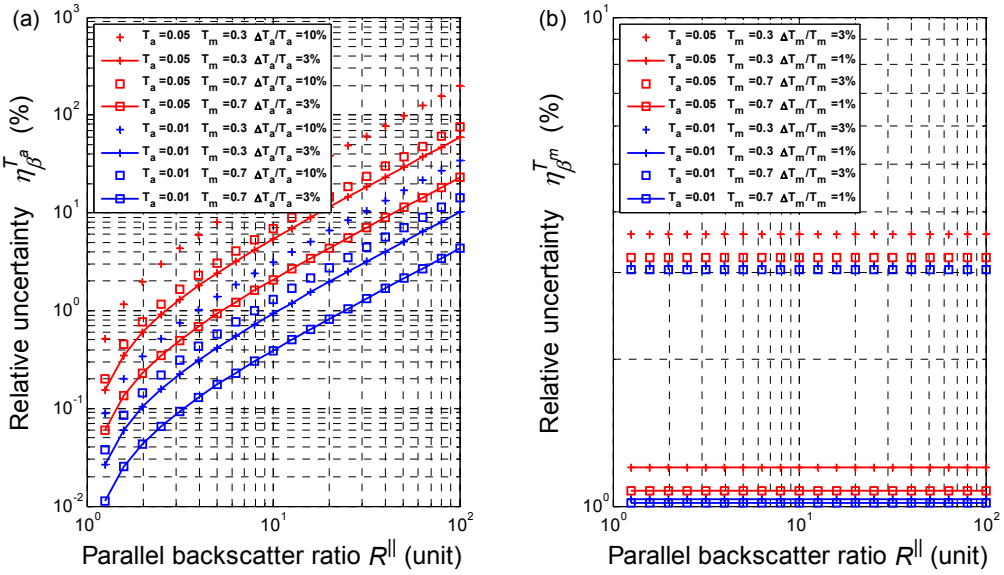

Fig. 3 The backscatter coefficient error resulted by the uncertainties of the spectral constants for different aerosol loading atmosphere, (a) only resulted from the determination error of T_a, (b) only resulted from the determination error of T_m.

Overall, when the aerosol loading is very small, the impact from ΔT_a is very small and the volume backscatter retrieval is limited by ΔT_m. However, when the aerosol loading is large, the contribution from ΔT_a dominates the retrieval error which increases as increasing ΔT_a.

Since the aerosol backscatter coefficient can be obtain by subtracting the known molecular backscatter coefficient from the total backscatter coefficient, the aerosol backscatter coefficient, β_a, has the same measurement error as the total backscatter coefficient, β. As already stated, the absolute uncertainty of optical depth follows the behavior of the relative uncertainties of the backscatter coefficient. But note that, the plots of the relative uncertainties in Fig. 3 share percentage longitudinal axes while the plots for the absolute uncertainties of optical depth should range from 10^{-4} to 10^{0}. For other parameters, the volume extinction coefficient which is the derivative of the optical depth for instance, the accuracy can be estimated from the relative uncertainty of the volume backscatter coefficient or the absolute uncertainty of the optical depth. But we should note that, the trends of the measurement accuracy are similar for all the detected parameters: smaller T_a and larger T_m both with better determination errors tend to produce better measurement accuracy. The T_m induced error plays more important role when the aerosol loading is very low while the impact of T_a dominate the measurement accuracy when the aerosol loading gets higher.

5. Conclusions

A polarized HSRL that employs an interferometric spectral filter and is under development at the Zhejiang University was introduced in this paper. The mathematical basis for the retrieval of the aerosol optical properties such as extinction-to-backscatter ratio, and aerosol depolarization ratio, extinction and backscatter coefficients were presented. Error analyses and sensitivity studies have been carried out on the transmittance characteristics of the spectral filter. The result shows that a filter that has as small aerosol transmittance (i.e., large aerosol rejection rate) and large molecular transmittance as possible is desirable. To achieve

#188635 - $15.00 USD Received 10 Apr 2013; revised 15 May 2013; accepted 16 May 2013; published 21 May 2013
(C) 2013 OSA

accurate retrieval, the transmittance of the spectral filter for molecular and aerosol scattering signals should be well characterized.

Acknowledgments

This work was partially supported by the National Defense Key Program of China (0205010803.18), the State Key Lab. of Modern Optical Instrumentation Innovation Program (MOI201208), the "985" III: First-Class Discipline Construction Program, and the Fundamental Research Funds for the Central Universities (2013QNA5006). The authors would like to express their great appreciation to the reviewers and the editor for the improvement of this paper.

#188635 - $15.00 USD Received 10 Apr 2013; revised 15 May 2013; accepted 16 May 2013; published 21 May 2013
(C) 2013 OSA